

# Peak and Post-Peak Shear Strength of Cement-Bentonite

**Paul J. Axtell, P.E.**, Dan Brown and Associates, Overland Park, Kansas;  
paxtell@danbrownandassociates.com

**Timothy D. Stark, Ph.D., P.E.**, University of Illinois

**John C. Dillon, P.E.**, U.S. Army Corps of Engineers, Kansas City District

## ABSTRACT

Self-hardening cement-bentontie (c-b) slurry walls were constructed as shear walls to stabilize the downstream slope of Tuttle Creek Dam near Manhattan, Kansas. The slope stabilization was required to protect the existing pressure relief well system located at the downstream toe of the dam. The wells require protection from slope deformation induced by liquefaction of the foundation sands during or immediately after the design seismic event. The shear walls are transverse to the axis of the dam, unreinforced, and relatively brittle members that may be exposed to relatively large shear strains, and possible cracking, during or immediately after shaking. An extensive laboratory investigation was conducted on recovered core samples to optimize the mix design and stabilization scheme. Furthermore, as is the topic of this paper, a portion of the laboratory investigation was to determine the large-strain, or post-peak, shear strength of the c-b material for use in limit-equilibrium slope stability analyses and numerical deformation modeling to assess the magnitude of permanent deformation caused by the design earthquake. These data may be beneficial to other projects that are considering the use of unreinforced c-b slurry walls for seismic retrofit purposes.

## INTRODUCTION

Tuttle Creek Dam, located on the Big Blue River in the Kansas River Basin, is part of a system that provides a comprehensive plan for flood control and other functions in the Missouri River Basin. The dam was designed and constructed by the US Army Corps of Engineers, Kansas City District in the 1950's. It is located about 10 km north of the city of Manhattan in eastern Kansas, as shown in Fig. 1.

The embankment is 2,300 m (7,550 ft) long and about 43 m (140 ft) high. A typical cross-section of the dam is shown in Fig. 2, identifying the general locations of the various embankment fill zones. The crest width is 15.2 m (50 ft) and the base width varies from about 430 to 490 m (1,400 to 1,600 ft). The top of the dam is at elevation 353.3 m (1,159 ft) while the original ground surface varies in elevation from about 310 to 313 m (1,017 to 1,027 ft) across the valley. Tuttle Creek Dam is a rolled earthfill dam; details of the fill zones and construction of the dam can be found in Lane and Fehrman (1960).

The main influential seismic source zones are the Nemaha Ridge uplift zone and the Humboldt Fault zone. The maximum credible earthquake (MCE) is a magnitude 6.6 event

at 20 km (12.5 miles) with a return period of about 3000 years. The peak horizontal ground acceleration, PHGA, of the MCE is 0.30g mean and 0.56g mean plus one standard deviation. The threshold liquefaction event is a magnitude 5.7 with a return period of about 1700 years. The Kansas City District found that rehabilitation of the liquefiable foundation sands is required to prevent an uncontrolled release of the reservoir during or after the design ground motion.



**[FIG. 1] General Location of Tuttle Creek Dam**

As part of the required seismic rehabilitation, transverse shear walls were constructed through the embankment and underlying foundation soils in the downstream slope and toe of the dam. Some preliminary design

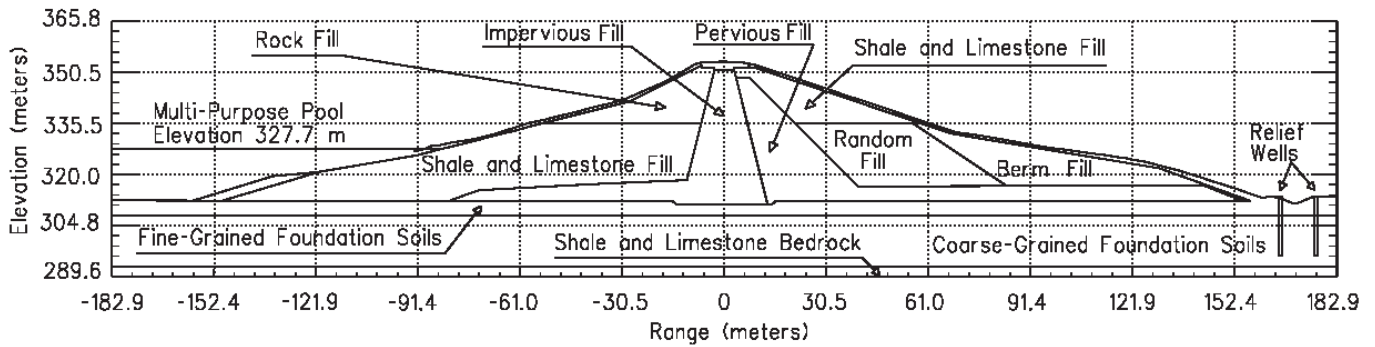


[FIG. 2] Typical cross-section of Tuttle Creek Dam

drawings depicting the plan and profile of these shear walls are shown in Figs. 3 and 4, respectively. The walls are 1.22 m (4 ft) wide, 13.72 m (45 ft) long, and generally about 21 m (69 ft) deep. A 3.05 m (10 ft) clear-space generally exists between them. Design of the clear-spacing considered requirements for unimpeded seepage between the walls in both the pervious drain and foundation sands, while also considering soil displacement between the walls using limit equilibrium methods. These transverse shear walls are self-hardening cement-bentontie (c-b) slurry walls, primarily excavated with a clam-shell. Note that slightly smaller walls were also excavated with a long-reach excavator early in the project for comparison purposes between the two construction methods. The c-b slurry walls are oriented perpendicular to the crest of the dam, unreinforced, and

relatively brittle members that will be exposed to relatively large shear strains during or immediately after the design seismic event. Such loading may crack the shear walls, after which the frictional resistance of the cracked section will govern the ability of the shear walls to resist gravitational forces induced by the slope. Large deformations at the downstream toe are not acceptable because of the presence

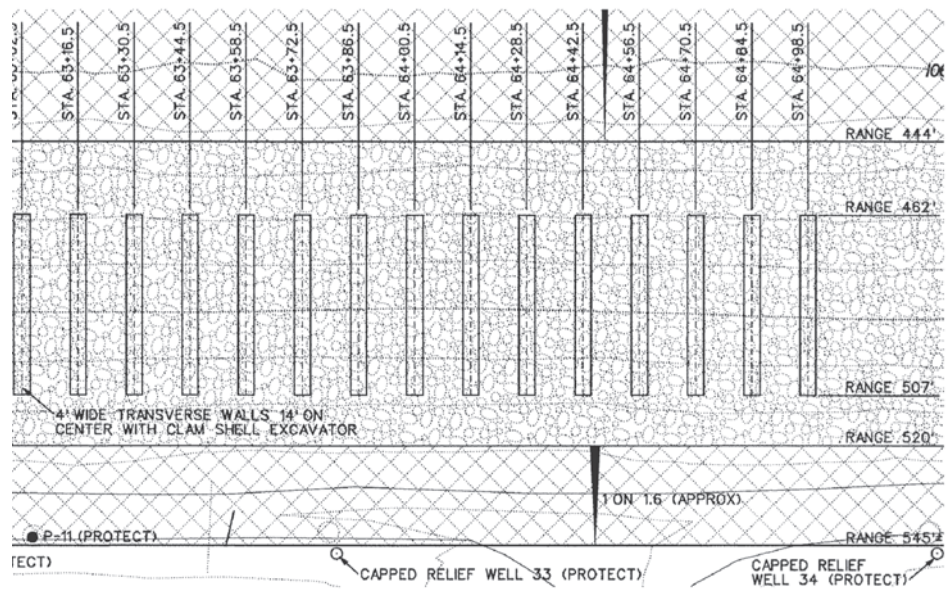


[FIG. 3] Plan View of Transverse Shear Walls (units in feet, 1 m = 3.28 ft)

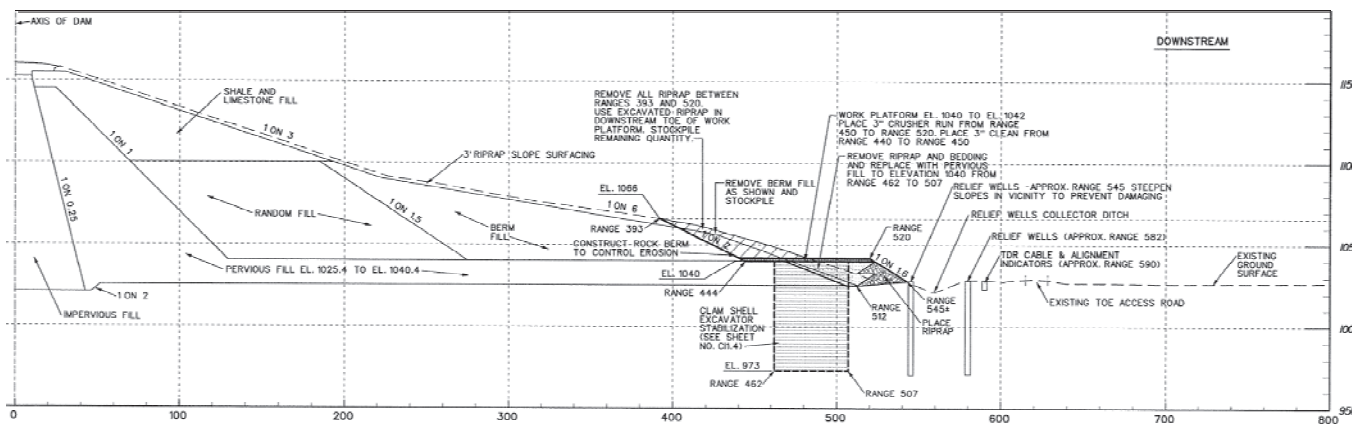


[FIG. 4] Profile View of Transverse Shear Walls (units in feet, 1 m = 3.28 ft)

of a fragile pressure relief well system. This relief well system provides vital underseepage pressure relief during operation of the reservoir and damage could lead to foundation erosion and piping.

A laboratory investigation was conducted on recovered samples obtained from production walls (initially they were test walls) to determine the large-strain, or post-peak, shear strength of the hardened cement-bentonite material. Testing included isotropically consolidated, undrained shear (R-bar) triaxial compression tests and drained direct shear tests. Testing was performed on samples that were recovered from walls constructed with cement-to-water (c/w) ratios of 0.3, 0.4 and 0.5. Both mixes include a 5 percent bentonite component. The results of the laboratory investigation were required for use in limit-equilibrium slope stability analyses used to design the shear walls and numerical deformation modeling to assess the earthquake induced permanent deformation of the dam and foundation materials. For the majority of the production work, unconfined compression tests were used to validate the design. The test results presented in this paper are for samples recovered from a test section that also serves as production shear walls. The testing presented herein was required for design.

## SOIL PROFILE

A working platform was constructed on the downstream slope of the dam to facilitate construction of the shear walls. The platform was constructed by: 1) removing the existing random fill material to expose the underlying pervious drain fill; 2) importing and placing sand (SP); and 3) placing approximately 60 cm (2 ft) of road sub-base for a working surface. The only portion of the embankment that the walls are in contact with is the pervious drain material downstream of the core, which lies above the natural cohesive blanket (ML and CL). The pervious drain material is composed of dense dredged SP soil, and is approximately 4.6 m (15 ft) thick.

The soils in the alluvial foundation of the dam consist of 2.4 to 8.2 m (8 to 27 ft) of silt and clay (natural cohesive blanket) underlain by sand, silty sand, and gravelly sand to a depth of 12.2 to 24.4 m (40 to 80 ft). The silt and clay form a natural cohesive soil blanket over the more permeable sands. This natural cohesive blanket is an important component of the

seepage control system for the dam, as are the pressure relief wells at the downstream toe. The sand deposits vary in thickness from about 7.6 to 18.3 m (25 to 60 ft) and can be separated into two distinct zones. The upper zone consists of a 4.6 to 6.1 m (15 to 20 ft) thick loose fine to medium sand (SM, SP, and SW) and the lower zone consists of a 7.6 to 9.1 m (25 to 30 ft) thick dense coarse to gravelly sand that increases in grain-size with depth (SP, SW, GP, GW). Due to the alluvial nature of the foundation deposit, multiple lenses of cohesive soil exist within the coarse-grained layers. The upper sand zone was determined to be potentially liquefiable during the design ground motion. The bedrock consists of alternating layers of shale and limestone (Permian age); however, the transverse shear walls do not penetrate bedrock. The c-b walls were keyed into the dense, coarse to gravelly sand and occasionally were founded on bedrock, particularly near the left abutment.

## SAMPLING AND TESTING

Wet-grab samples were cast in 7.6 cm by 15.2 cm (3 in by 6 in) cylinders and stored underwater until testing was performed. The grab sample was obtained from a shear wall shortly after construction and before the slurry hardened. After hardening, the shear walls were cored and the resulting core samples were also stored underwater until testing was performed. Wall coring was conducted with the Geobore system (double-barrel wireline) producing 10 cm (4 in) diameter samples. Coring was conducted about three weeks after construction of the walls. Testing was conducted at least 70 days after construction.

Based on an independent laboratory investigation of the proposed mixes, and verified by full-scale field measurements, relatively minor strength increases can be expected beyond 90 days for these materials. The majority of the tests occurred within the 90 day time frame. A significant unconfined compressive strength discrepancy between the wet-grab and core sample strength was observed at higher c/w ratios as described by Axtell, et al. (2009).

## INTERPRETATION OF TEST RESULTS

Testing included isotropically consolidated, undrained shear (R-bar) triaxial compression tests and drained direct shear tests. The tests were performed by Kleinfelder, in Topeka,



Kansas. The post-peak or ultimate strength measured on core samples via R-bar and direct shear tests was taken into consideration during the design of these walls for the seismic retrofit because some cracking of the walls is expected during the design ground motions. Thus, the peak strength of the hardened shear walls would not be operational, i.e., would have been exceeded due to cracking of the walls. The results of the R-bar tests are provided below, along with the results from the direct shear tests.

### R-BAR SHEAR RESULTS

The R-bar tests were performed on 6.6-cm (2.5 in) diameter samples with heights ranging from 11.5 to 14.5 cm (4.5 in to 5.7 in). R-bar tests were conducted on recovered core samples from walls constructed by both the clam-shell and long-reach excavation methods. Trimming of the samples was achieved by re-coring the selected specimens to the proper diameter. It is unknown if the trimming process had any effect on the results. In addition, two suites of tests were conducted on wet-grab samples from clam-shell constructed walls. Three of the samples were from walls constructed with a c/w ratio of 0.4 and one with a c/w ratio of 0.3. The remaining six samples were obtained from walls constructed with a c/w ratio of 0.5. Total stress failure envelopes for peak and post-peak strength were determined, as was the effective stress failure envelope for post-peak strength. All failure envelopes were determined by testing separate samples at confining stresses of 69,

207, and 552 kPa (10, 30 and 80 psi), which are thought to adequately encompass the expected in-situ stress range. The strain rate for all of the tests was 0.08 mm/min (.003 in/min). This rate was chosen to facilitate drainage of excess pore pressures generated during shear and was estimated based on consolidation test results. Each specimen was tested to the maximum axial strain practical, which was usually less than 20 percent in the R-bar tests. A common constraint was ripping or tearing of the specimen membrane during shear due to the sharp pieces of concrete from the specimens. Post-peak values were obtained at the maximum axial strain measured (excluding data after a membrane tear occurred). The results of the tests are summarized in Table 1. The values of dry unit weight, moisture content, and void ratio provided in Table 1 are average values for the three specimens tested at each location (three data points are used to define the failure envelope). The moisture contents reported in Table 1 are from portions of the specimen collected after the shearing phase of the test. Generally, but not always, the moisture content of the samples decreased by around 5 percent during the consolidation phase of the test. Back-pressure saturation was utilized; the mean B was 0.96, with a standard deviation of 0.05.

Deviator stress versus axial strain relationships for the 15 specimens of c/w=0.5 core samples (five suites of tests, each with three points associated with the three different confining stresses) are provided in Fig. 5. The results of tests conducted on c/w=0.4 walls are not

[TABLE 1] R-bar results (both total and effective stress).

Core Hole	Excavation method	Sample Depth (m)	c/w ratio	Dry Unit Weight (kN/m <sup>3</sup> )	Moisture Content (%)	Void Ratio	Strain at Peak (%)	Peak		Post-Peak		Post-Peak	
								c	Φ	c	Φ	c'	Φ'
								(kPa)	(°)	(kPa)	(°)	(kPa)	(°)
VC06	Long Reach	19.8	0.3	10.36	68	1.68	1.3	276	36	255	34	0	51
VC08	Clam-Shell	9.1	0.4	9.11	69	2.03	2.4	593	0	476	0	0	46
		19.8	0.4	12.09	45	1.44	2.2	310	41	407	30	0	51
VC05	Long Reach	9.1	0.5	10.21	60	1.71	0.7	538	29	421	22	0	45
C-958		19.8	0.5	12.40	42	1.22	0.8	1151	18	731	25	0	49
VC14	Clam-Shell	9.1	0.5	10.99	48	1.52	1.6	352	37	262	39	0	46
VC17		15.2	0.5	10.21	57	1.69	0.6	931	8	434	17	0	46
		19.8	0.5	10.68	54	1.58	0.9	690	27	310	34	0	46
Wet Grab		15.2	0.4	9.11	66	2.04	0.9	986	7	207	30	0	46
		13.7	0.5	10.83	56	1.55	0.9	1655	12	807	27	0	50

shown, nor are the wet-grab results. The production walls are to have a  $c/w=0.5$  so the  $c/w = 0.4$  results are not relevant and data from core testing was being used for the design and acceptance criteria; hence, those were the samples used for design. The linear line super-imposed on Fig. 5 indicates the stress-strain relationship modeled in the permanent deformation analyses performed using FLAC (Itasca, 2000). The post-peak, or large-strain, strength of core samples of  $c/w=0.5$  walls exceeds that required by the design. The measured initial stiffness is also somewhat greater than modeled (average initial Young's modulus equals 538 MPa (78 psi) with a standard deviation of 148 MPa (21.5 psi)) but the majority of the stress-strain relationships still indicate stronger material than modeled in the FLAC analyses. Thus, the permanent deformations estimated after wall cracking using FLAC are probably conservative and within allowable values.

The change in pore pressure during shear versus axial strain is shown in Fig. 6 for the 15 specimens of  $c/w=0.5$  core samples. As expected from the relatively high void ratios measured prior to shear, all samples tended to initially generate high positive pore pressures. At higher axial strains, the excess pore pressures became negative for all 10 specimens tested at the lower confining stresses (69 and 207 kPa or 10 and 30 psi), whereas the 5 specimens at the higher confining stress (552 kPa or 80 psi) remained positive.

Note that the actual strain values are reported on the x-axis in Figs. 5 and 6 ( $\Delta l/l$ ) whereas the corresponding values in Table 1 have been reported as a percentage.

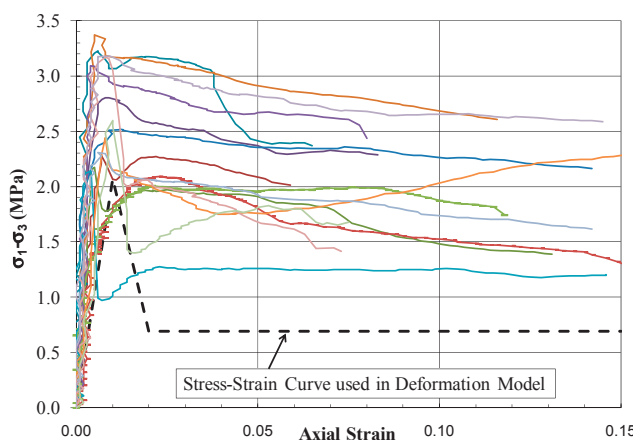


**[FIG. 5] Stress-strain relationships from R-bar tests on  $c/w = 0.5$  core samples (both long-reach and clam-shell excavators, at all confining stresses) and relationship used in FLAC deformation analyses.**

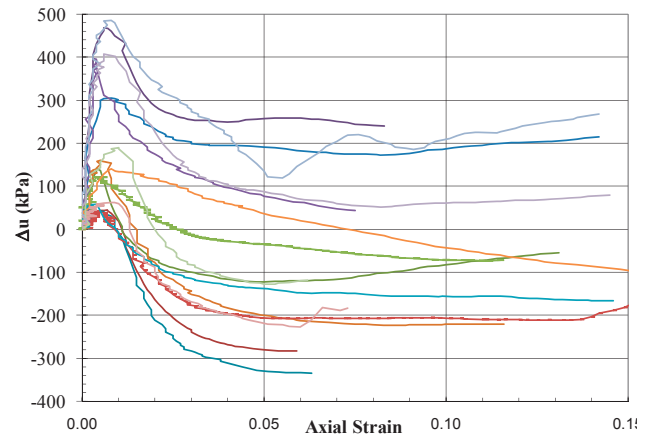


**[FIG. 6] Pore pressure change versus axial strain from R-bar tests on  $c/w = 0.5$  core samples (both long-reach and clam-shell excavators, at all confining stresses).**

## DIRECT SHEAR RESULTS

The direct shear tests were performed on 6.35-cm (2.5 in) diameter samples with a height of 2.54 cm (1 in). All direct shear tests were conducted on recovered core samples from shear walls constructed by the clam-shell excavation method. Trimming of the samples was achieved by re-coring the selected specimens to the proper diameter. It is unknown if the trimming process had any effect on the results. The tests were performed by Kleinfelder in Topeka, Kansas. Three of the samples were obtained from walls constructed with a  $c/w$  ratio of 0.4. The remaining six samples were from walls constructed with a  $c/w$  ratio of 0.5. Failure envelopes for peak and post-peak strength were normal stresses of 96, 192, 384, and 574 kPa (14, 28, 56 and 83 psi). The shear displacement rate for all of these tests is 0.005 mm/min (0.0002 in/min). This rate was chosen to facilitate drainage of excess pore pressures generated during shear based on consolidation test results. Each specimen was tested to a 0.64 cm (0.25 in) horizontal displacement. Post-peak strength values were obtained at the maximum horizontal displacement (0.64 cm) (0.25 in), whereas the peak values were generally observed at a horizontal displacement of less than 0.25 cm (0.1 in). The results of these tests are summarized in Table 2. The values of dry unit weight, moisture content, and void ratio provided in Table 2 are average values for the four specimens tested at each location (four data points defining the failure envelope).

Approximately three-quarters of the 36 specimens (9 tests, each with four normal stresses) show a slight contraction initially, after which the specimens began to dilate. Initial contraction on the order of about 0.5

[TABLE 2] Direct shear results (Clam-Shell Constructed Walls and Core Samples).

Core Hole	Sample Depth (m)	c/w ratio	Dry Unit Weight (kN/m <sup>3</sup> )	Moisture Content (%)	Void Ratio	Peak		Post-Peak	
						c' (kPa)	Φ' (°)	c' (kPa)	Φ' (°)
VC08	9.1	0.4	8.01	76	2.5	172	44	21	41
	15.2	0.4	9.26	63	1.8	400	56	110	60
	19.2	0.4	9.73	60	1.8	296	37	41	39
VC17	3.7	0.5	8.16	79	2.4	303	33	48	36
	4.6	0.5	8.64	79	2.4	386	20	193	23
	6.1	0.5	8.64	76	2.2	276	32	14	42
	9.1	0.5	8.64	72	2.0	400	25	97	27
	12.2	0.5	8.95	71	2.1	241	41	28	37
VC14	15.5	0.5	9.89	59	1.7	352	40	62	40

percent of the original sample height was common whereas dilation on the order of 0.5 to 5 percent was observed with increasing horizontal displacement. Opposite behavior was observed for the remaining one-quarter of the specimens. Unfortunately, no discernable trend was apparent between volumetric change and c/w ratio, depth, void ratio, moisture content, or dry unit weight.

The two upper samples from core hole VC08 indicate effective friction angles that are noticeably higher than the other samples, both at peak and post-peak. The exact reason for the phenomenon is not known, but expected to be a result of the presence larger or more angular natural soil particles in the sample. The R-bar results from VC08 do not appear to validate or dispel this conclusion.

The effective cohesion and effective friction angle versus depth as determined by direct shear testing are provided in Figs. 7 and 8, respectively. These figures only present the results of tests conducted on samples with a c/w ratio equal to 0.5, because the production work is utilized for this mix. Also included in Figs. 7 and 8 are the mean, mean minus one standard deviation, and mean plus one standard deviation for each data set. Based on these figures, there does not appear to be a discernable trend between shear strength and depth in the shear wall. The presence of a post-peak cohesion value indicates that the shear displacement imposed in the direct shear tests was not sufficient to reach a residual strength condition.

Unlike soil, there also does not appear to be a distinct relationship between void ratio and

shear strength, as shown in Fig. 9. This seems apparent for the effective cohesion and friction angle at both peak and post-peak values.

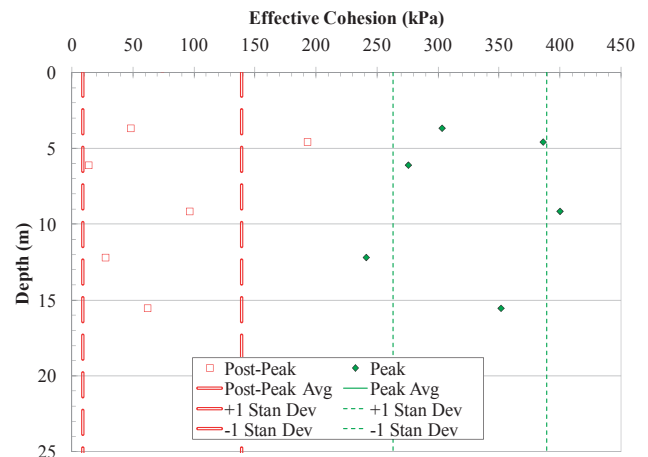


[FIG. 7] Direct shear effective cohesion versus depth in shear wall for c/w=0.5 samples.

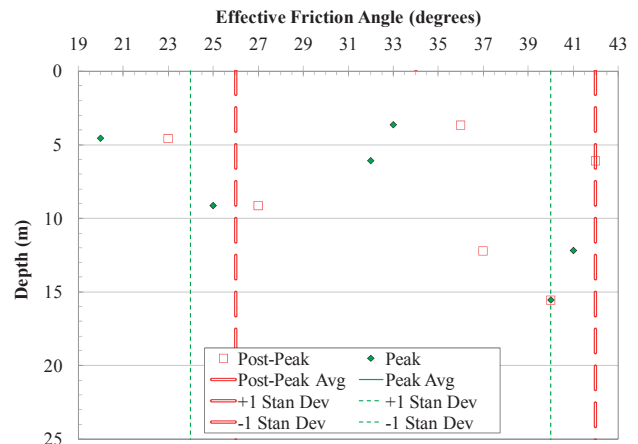


[FIG. 8] Direct shear effective friction angle versus depth in shear wall for c/w=0.5 samples.

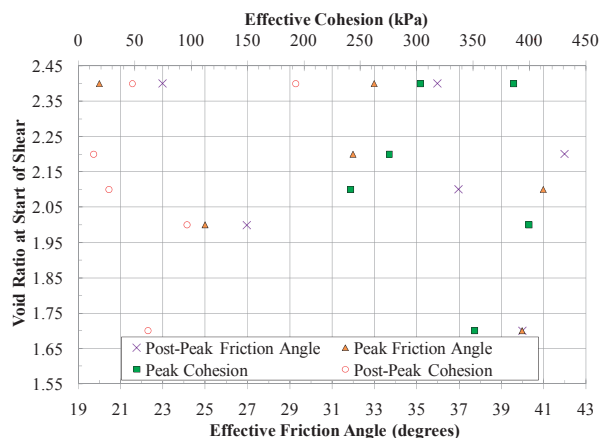


**[FIG. 9] Direct shear strength parameters versus void ratio for  $c/w=0.5$  samples (all cored samples, constructed with clam shell excavator).**

## REPRESENTATION OF TEST RESULTS IN ANALYSES

The data presented herein was used to estimate a strength and modulus profile for the depth of a transverse shear wall to model the variation in strength and stiffness with depth in the FLAC analyses. Results from both the R-bar and direct shear tests were considered in determining the strength and stiffness design values. However, results from the R-bar tests were more heavily relied upon as a result of the forced failure plane orientation in the direct shear tests, as well as questions resulting from the somewhat limited magnitude of the direct shear test displacements. Based on this data, the following average stress-strain behavior was used in the deformation analyses:

1. Peak strength (total stress):  $c = 655$  kPa (95 psi) and  $\phi = 24^\circ$ .
2. Post-peak strength (effective stress):  $\phi' = 46^\circ$ .
3. Young's modulus (tangent):  $E = 496$  MPa (72 ksi).
4. Peak strength attained at axial strain:  $\epsilon = 0.8\%$
5. Post-peak strength begins at axial strain:  $\epsilon = 1.6\%$ .

This characterization may be beneficial to other projects that are trying model the seismic performance of shear walls.

## CONCLUSIONS

Cement-bentonite (c-b) self-hardening slurry walls were constructed as a seismic retrofit of the downstream slope of Tuttle Creek Dam. Post-peak, or large-strain, shear strength will likely dictate the performance of these

unreinforced walls during or following the design seismic event due to cracking of the walls during shaking. Laboratory R-bar and direct shear testing of recovered core and wet-grab samples was conducted to evaluate both peak and post-peak strength for use in the wall design and estimate of post-earthquake permanent deformations. The results of the laboratory testing program are presented and indicate that a  $c/w=0.5$  mix that includes a 5 percent bentonite component will meet or exceed the peak and post-peak strength requirements dictated by the design. These data may be beneficial to other projects that are considering the use of unreinforced c-b slurry walls for seismic retrofit purposes.

## ACKNOWLEDGMENTS

The contents of this paper are the authors' and do not necessarily reflect those of the represented entities. The authors acknowledge the support provided by the U.S. Army Corps of Engineers - Kansas City District and Kleinfelder. The authors are particularly appreciative of the efforts by Joe Topi, Francke Walberg, Bill Empson, and David Mathews. Finally, the expertise of the contractor, Treviicos South, was essential.

## REFERENCES

1. Axtell, P.J., Stark, T.D., and Dillon, J.C. (2009). "Strength Difference between Clam-Shell and Long-Reach and Excavator Constructed Cement-Bentonite Self-Hardening Slurry Walls." *Contemporary Topics in Ground Modification, Problem Soils, and Geo-Support, ASCE Geotechnical Special Publication No. 187*; Iskander, Laefer, and Hussein, editors.
2. Itasca Consulting Group, Inc. (2000). *FLAC - Fast Lagrangian Analysis of Continua*, version 4.0, Itasca Consulting Group, Inc., Minneapolis, MN.
3. Lane, K.S., and Fehrman, R.G. (1960). "Tuttle Creek Dam of Rolled Shale and Dredged Sand." *Journal Soil Mechanics and Foundation Division*, ASCE, 86(SM6). 11-34.